

Electronic supplementary information

The surface areas of the BNKT nanoparticles were determined using the Brunaeur-Emmett-Teller (BET) N_2 adsorption/desorption isotherms method. The specific surface area of BNKT1, BNKT2 and BNKT3 nanoparticles are 15.45, 17.98 and 8.81 m^2/g respectively. Obviously, the surface areas of BNKT1 and BNKT2 are about twice that of BNKT3, which also contributes in part to the higher piezocatalytic performance of BNKT1 and BNKT2.¹

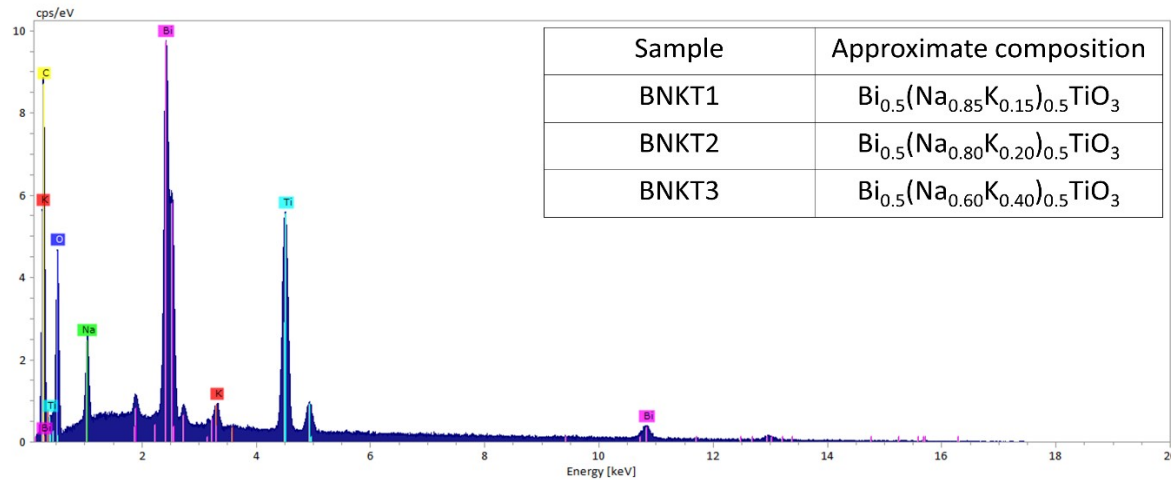


Fig. S1. The EDS spectra of BNKT2 nanoparticles. The inset Table gives the approximate compositions of the BNKT nanoparticles.

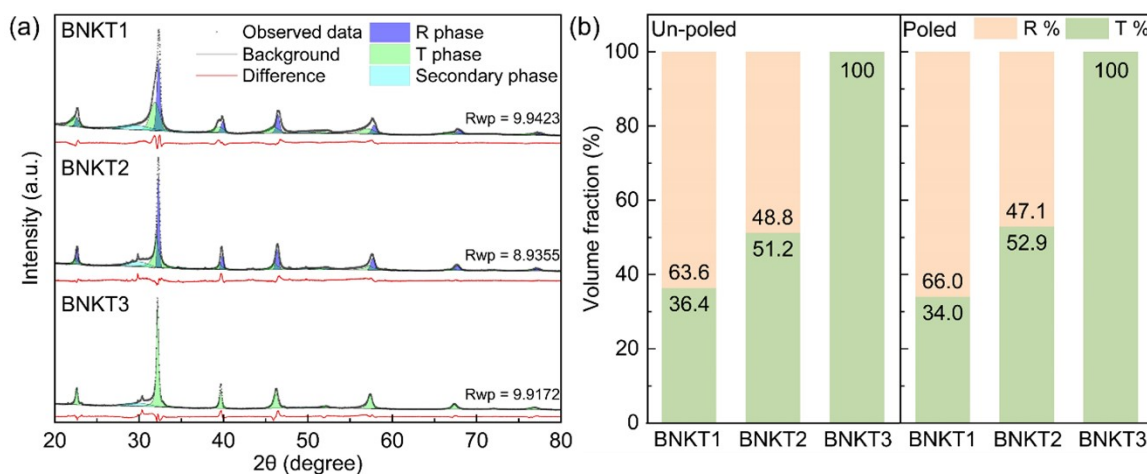


Fig. S2. (a) Rietveld fitted XRD patterns of unpoled BNKT1, BNKT2 and BNKT3 sample. (b) The volume fraction of rhombohedral and tetragonal phases in BNKT nanoparticles before and after poling.

Table. S1. The Rietveld refined lattice parameters of BNKT nanoparticles before poling.

Samples	BNKT1	BNKT2		BNKT3	
Structure	Tetragonal	Rhombohedral	Tetragonal	Rhombohedral	Tetragonal
Volume fraction (%)	36.4	63.6	51.2	48.8	100
Space group	P4mm	R3c	P4mm	R3c	P4mm
a (Å)	3.92381	5.49268	3.92996	5.52727	3.92816
b (Å)	3.92381	5.49268	3.92996	5.52727	3.92816
c (Å)	3.95281	13.5242	3.9472	13.5377	3.95038
Alpha (°)	90	90	90	90	90
Beta (°)	90	90	90	90	90
Gamma (°)	90	120	90	120	90

Table. S2. The Rietveld refined lattice parameters of BNKT nanoparticles after poling.

Samples	BNKT1	BNKT2		BNKT3	
Structure	Tetragonal	Rhombohedral	Tetragonal	Rhombohedral	Tetragonal
Volume fraction (%)	34.0	66.0	52.9	47.1	100
Space group	P4mm	R3c	P4mm	R3c	P4mm
a (Å)	3.92058	5.5167	3.92273	5.50905	3.92711
b (Å)	3.92058	5.5167	3.92273	5.50905	3.92711
c (Å)	3.95539	13.4424	3.95116	13.5514	3.95329
Alpha (°)	90	90	90	90	90
Beta (°)	90	90	90	90	90
Gamma (°)	90	120	90	120	90

Compared to our previous ^{23}Na NMR measurements on BNKT type materials,² where discontinuities observed in the NMR spectrum clearly indicate distinct sodium environments, in the present case the spectra yield an overall more uniform environment which can be attributed to the post-synthetic annealing step at 700 °C. On the other hand, compared to solid solutions (from solid state synthesis) of similar compositions,³ where the broad asymmetric NMR lineshapes can be fit with a single Gaussian Isotropic model (GIM-with the so called Czjzek distribution),⁴ in the present case the 1D spectra in Fig. 3a cannot be satisfactorily fit with only one or two GIM lineshapes. As such the present materials sit in between the high surface area un-annealed hydrothermal materials (200 °C) and the high temperature solid state synthesized materials (>1000 °C).

Table S3. Fitting Parameters of 1D slices from the ^{23}NA MQMAS NMR using DMFIT software⁴

Sample	Slice	Model	Position (ppm)	δCS (ppm)	CQ (kHz)	ηQ
BNKT1	(i)	Q mas 1/2	-13.5		1609.71	0.63
		CzSimple	-15.72	0.47	743.85	
	(ii)	CzSimple	-12.43	0.46	1011.71	
		CzSimple	-10.45	0.4	908.91	
		CzSimple	-10.97	0.6	1177.75	
		CzSimple	-13.8		1609.71	0.63
BNKT2	(i)	CzSimple	-16.47	0.5	567.53	
		CzSimple	-13.86	0.43	778.94	
	(ii)	CzSimple	-11.15	0.44	894.46	
		CzSimple	-11.66	1.07	950.43	
		CzSimple	-14.3		1609.71	0.63
BNKT3	(i)	CzSimple	-17.2	0.49	518.85	
		CzSimple	-15.04	0.45	778.94	
	(ii)	CzSimple	-11.78	0.35	831.79	0.47
		CzSimple	-12.19	0.99	844.47	0.62

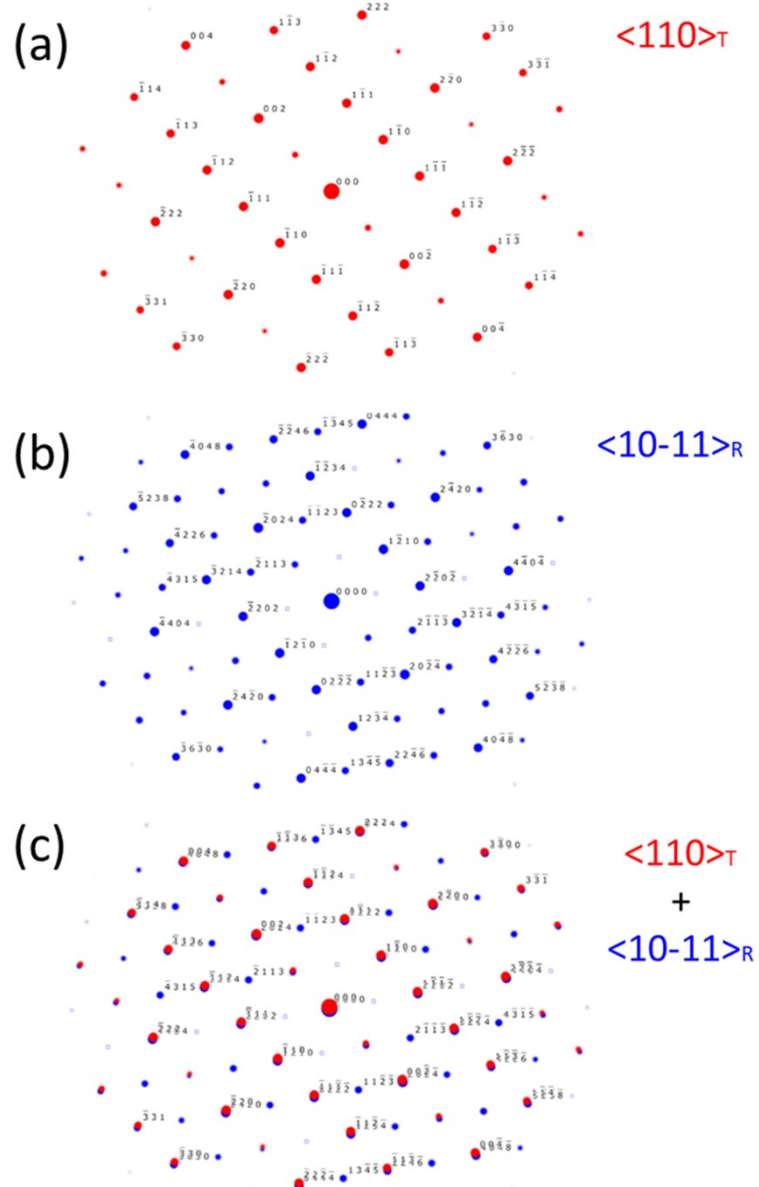


Fig. S3. Simulated SAED patterns along (a) [110] (b) [10-11] and (c) both [110] and [10-11] directions of BNKT2 nanoparticles.

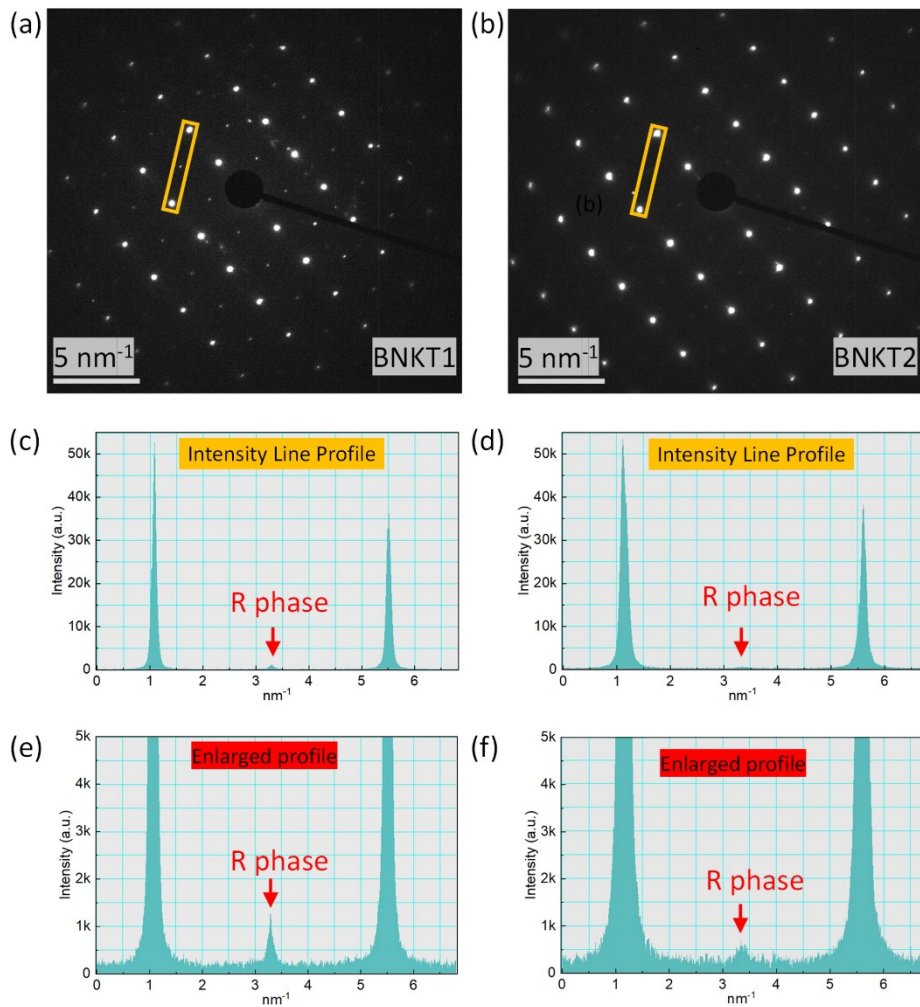


Fig. S4. SAED pattern of (a) BNKT1 and (b) BNKT2. The intensity line profile of the area encircled by the yellow boxes: (c) BNKT1 and (d)BNKT2. The normalized intensity profile of (e) BNKT1 and (f) BNKT2.

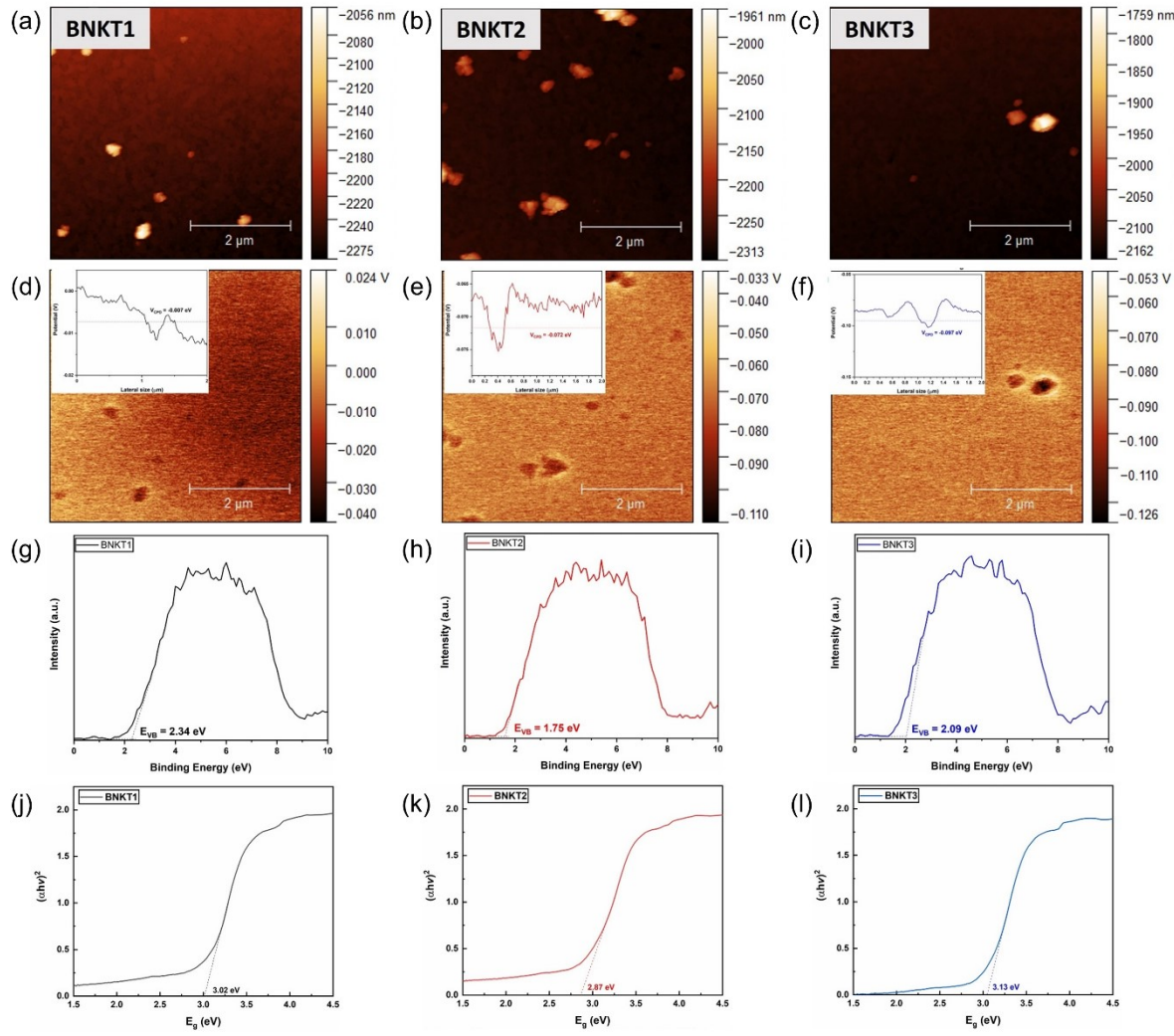


Fig. S5. (a)-(c) Surface topographic images by atomic force microscopy, (d)-(f) Contact potential difference by KPFM, (g)-(i) Kubelka–Munk plots from UV-vis reflectance spectrophotometry data, and (f)-(l) XPS valence band plots of BNKT1, BNKT2, and BNKT3 nanoparticles, respectively.

Reference

- 1 D. Liu, C. Jin, F. Shan, J. He and F. Wang, ACS Applied Materials & Interfaces, 2020, 12, 17443-17451.
- 2 M. B. Ghasemian, A. Rawal, Y. Liu and D. Wang, ACS Applied Materials & Interfaces, 2018, 10, 20816-20825.
- 3 K. Anjali, T. G. Ajithkumar and P. A. Joy, Materials Research Bulletin, 2019, 118, 110506.
- 4 D. Massiot, F. Fayon, M. Capron, I. King, S. Le Calvé, B. Alonso, J.-O. Durand, B. Bujoli, Z. Gan and G. Hoatson, Magnetic Resonance in Chemistry, 2002, 40, 70-76.